INSTITUTE OF PHYSICS PUBLISHING JOURNAL OF PHYSICS: CONDENSED MATTER

J. Phys.: Condens. Matter **14** (2002) 193–209 PII: S0953-8984(02)28789-5

Critical current in granular superconductor C–Si–W with peak-type re-entrant superconductivity

S M Chudinov[1], G Mancini[1], M Minestrini[1], R Natali[1], S Stizza[1] and A Bozhko[2]

[1] INFM, UdR Camerino, Dipartimento di Matematica e Fisica, Università degli Studi di Camerino, Via Madonna delle Carceri, 62032 Camerino (MC), Italy
[2] Moscow State University, 117234 Moscow, Russia

Received 5 September 2001, in final form 12 November 2001
Published 13 December 2001
Online at stacks.iop.org/JPhysCM/14/193

Abstract

Some granular disordered superconductors, namely diamond-like carbon–silicon films containing tungsten, show one or more small, clearly detectable peaks in resistivity curves at lower temperatures than that of the superconducting main transition, T_c. Based on the concept of cluster superconductivity and on the percolation theory, we carried out extensive numerical simulations that relate the appearance of the peak-type re-entrant superconductivity to the absence of superconducting percolative paths crossing the entire sample. The numerical determination of such paths allowed us to compute the maximum supercurrent density j_c to flow through the sample in the temperature region below T_c.

1. Introduction

Re-entrant and quasi-re-entrant superconductivity phenomena have drawn much interest from a theoretical and applicative point of view.

For the former, the interest shown for these phenomena is due to their fundamental importance in highlighting new aspects of the quantic nature of electrons in solids. In fact, the study of these effects enabled the discovery of several antagonistic mechanisms to superconductivity: magnetic ordering, clustering (decreasing the volume and total energy of the superconducting phase by charge carrier localization), electrostatic energy increase and decrease of the superconducting coupling of the system.

For the latter, the study of re-entrant phenomena provides additional important information on Josephson junction array (JJA) properties. A re-entrant superconductivity transition has been observed, for the first time, in magnetic superconductors of the type $HoMo_6S_8$ and $ErRh_4B_4$ [1], in which re-entrance came from the concurrence of magnetic ordering and superconductivity. This observation of a new effect in magnetic superconductors has offered the possibility of studying the various experimental situations that can occur, i.e. coexistence between the two phenomena or destruction of the superconducting phase. The extremely

different re-entrant transitions of the superconductor–dielectric type have been observed and studied in granular metallic systems (Al, Ga, In, Bi, etc) at temperatures $T < T_c$, demonstrating electron localization on single grains [2, 3].

Usually non-homogeneous materials are modelled as systems consisting of metal grains embedded in an insulating matrix [4–6]. In this case the superconductivity may be considered homogeneous when $\zeta < \xi$, where ξ is the effective superconducting coherence length of the medium and ζ is the correlation length characterizing the proximity of the system to the percolation threshold; for $\zeta > \xi$ the superconductivity is essentially inhomogeneous. If ξ is greater than the metal grain size, then the superconducting phase may be expected to be characterized by strong spatial fluctuations of the local critical temperature determined by the value of the correlation length ζ for the infinite conducting cluster; the superconducting phase can then be modelled as consisting of superconducting grains having different critical temperatures. When temperature decreases, the total volume of the superconducting phase increases; when it reaches the percolation threshold an infinite cluster is formed and a superconducting transition occurs.

Despite experimental evidence [2, 3, 7–13], there is still some dispute whether granular superconductors can show the re-entrance phenomenon.

The first theoretical analysis of re-entrant phenomena in granular superconductors has been executed by Abeles, Šimanek and Efetov [14–16]. They reproduced the experimental situations taking into account the self-capacitances of the grains, but subsequent improvements gave different results; accordingly, they took into account the interplay of self-capacitances, inter-granular capacitances and the presence of charge excess on grains [17].

Let us underline that the theoretical analysis of the superconducting–dielectric transition at temperatures $T < T_c$ has been presented only for a periodic system, in which the metallic grains are placed at the vertices of a crystal lattice. According to the theoretical analysis, at low temperatures these systems are governed by the competition between two energies E_C and E_J. For a couple of grains i, j, E_C is the energy of the Coulombian blockage

$$E_C^{i,j} = \frac{1}{2}\frac{Q_i Q_j}{C_{ij}} \tag{1}$$

(Q_i, Q_j represent the charge excesses for grains i and j, respectively, both when self-capacitances ($i = j$) or inter-granular capacitances ($i \neq j$) are considered) and E_J is the characteristic energy of Josephson coupling for nearest-neighbouring grains ($i = j \pm 1$)

$$E_J^{i,j}(T) = \frac{\pi\hbar}{4e^2}\frac{1}{R_N^{i,j}}\Delta(T)\tanh\left(\frac{\Delta(T)}{2k_B T}\right) \tag{2}$$

with $\Delta(T) = \Delta(0)(1 - T/T_c)^{\frac{1}{2}}$ giving the superconducting gap $\Delta(T)$ at temperatures $T < T_c$, where $\Delta(0)$ is the gap at $T = 0$ K, e the charge of a single electron, $\hbar$ the Planck constant, k_B the Boltzmann constant and $R_N^{i,j}$ the resistance for a single electron tunnelling between neighbouring grains [31]. The phase diagram showing the transition confinement from superconducting to dielectric state in disordered JJA has been mapped in the plane $k_B T_c/z\bar{E}_J - E_C/z\bar{E}_J$ (for z nearest-neighbouring grains) [15–17]. The analysis developed in these works is able to describe the main features of the superconducting–dielectric transitions observed in granular metal systems like Al, In, Ga, Bi, etc. This analysis predicts that granular metals remain in the dielectric state at low temperatures $T \to 0$ K. In recent years much experimental and theoretical interest has been manifested for two-dimensional periodical networks artificially fabricated by planar technology (see [18, 19] and references therein). These are ordered systems and may be better described by the theoretical analysis developed in [15–17] for a periodic JJA.

During the last decade a new class of granular superconductors has been found consisting of grains of transition metals (W, Mo, Nb, Cr) immersed in a diamond-like carbon–silicon dielectric matrix [20–22]. The system C–Si–W has been studied in detail, and it has shown a new quasi-re-entrant phenomenon that manifests as small peaks of resistance $\Delta(R) \sim 10^{-3} R_n$ (R_n being the normal resistance immediately over T_c) extending for $\Delta(T) \sim 0.1$ K

In the C–Si–W system one or two peaks have been observed in the temperature range $1\ \mathrm{K} < T < T_c$; for $T < 1$ K the system remains in the superconducting state at least down to 16 mK [22, 23]. The C–Si–W system manifests a quasi-re-entrant phenomenon, since besides the main superconducting transition—sometimes incomplete— a non-zero resistance also appears in the temperature regions bounded by the main superconducting transition and the peaks themselves [22–25]. This quasi-re-entrant phenomenon is indicated as the 'peak-type' one. Experimental study demonstrates that quasi-re-entrant peaks are not observed in magnetic susceptibility (χ) measurements carried out using a resolution $\Delta(\chi)/\chi \sim 10^{-3}$ [26]. The superconducting main transition in susceptibility $\chi(T)$ is shifted by ∼1.5 K towards zero with respect to the main transition in resistance $R(T)$ (figures 2 and 3 in [26]) and a strong non-ohmic behaviour is observed in the proximity of the peaks [24, 25]. The critical magnetic field for quasi-re-entrant peaks is always less than that of the main superconducting transition. In a recent paper [26] we proposed and analysed the possible mechanisms of the re-entrant 'peaks-type' transitions. These mechanisms are based on the Coulombian blockage (superconductor–insulator transition) and on the Josephson coupling unblockage (insulator–superconductor transition). The proposed mechanisms have been successfully used for the numerical simulation of the re-entrant 'peaks' position on the temperature scale for one and two peaks cases. The present paper is devoted to the experimental measurements of the critical current for macroscopic samples and to the numerical simulation of the critical current in a single current path and for all superconducting paths in the bulk superconductor. 'Peak-like' re-entrant phenomena properties are summarized in [26]. It is important to pay attention to the fact that in our samples the resistance of the peak is very small (amounting to units of $\mu\Omega$ cm). In other words the blockage of the superconducting current regards only a relatively small number of grains among the ones forming the infinite superconducting cluster. This means that the re-entrant phenomenon has a local mesoscopic character and cannot be analysed as a transition involving the whole system. In contrast with other systems, in our samples the network of superconducting grains is disordered, with the grain radii and distances randomly distributed around some mean values. That is the reason why a numerical simulation is more appropriate than a theoretical analysis to investigate the sample behaviour. According to our intentions, the numerical simulation should reproduce all the experimental characteristics shown by our samples: the peaks' existence, their behaviour in a magnetic field, the strong non-ohmic characteristics. At the moment, the numerical simulation has been able to prove the existence of one or two peaks and allowed the calculation of the superconducting critical current j_c. The former result has been illustrated in a previous work of ours [26], the latter is the object of this paper.

2. Experimental

Films of the C–Si–W system with thickness about 0.5 μm were grown on polycrystalline dielectric substrates (thickness about 250 μm) using plasma decomposition of organosiloxane vapours in a dc diode reactor. Tungsten, whose concentration x could reach about 40%, was introduced into the growing film using magnetron sputtering. Details on the growth process can be found in [20–22]. All specimens consisted of films 2 mm long, 2 mm wide and 0.5 μm thick (giving a section of 10^{-5} cm^2), with tungsten concentration varying from 5–10 to 40

at.%; contacts to the films were prepared using silver paint. In order to improve their adhesion and stability to the thermocycling in a wide temperature range, the films with prepared contacts were heated up to 200–250 °C over a period 10–15 min. Such a treatment does not lead to any change in the structural and electrophysical properties of the investigated films [20, 22]. The electroconductivity measurements were performed by the application of the usual four-terminal technique both in dc and ac lock-in regimes [22]; the susceptibility measurements were carried out using an astatic coil magnetometer in a magnetic field perpendicular to the films. Low-angle electron and x-ray diffractions confirmed the amorphous structure of the films for all tested compositions. The analysis of the emission spectrum of a W-edge coated with a diamond-like film proved the absence of ordering in the structure. At low concentration, silicon and transition metals enter the α-C–Si matrix in their free elemental form. The metal presence in the films consists of uniformly dispersed small-particles clusters. Using transition metals one has to deal with a complex system made up of polymer, metal, metal carbide, metal silicide and even metal oxide when no diffusion barrier is deposited on the film surface to prevent post-deposition oxidation. The electrical and superconducting properties of such a composite system, with different concentrations of tungsten, are determined by percolation among metallic clusters in a uniform dielectric polymer matrix and have been studied in detail in [20, 22]. In principle, the superconducting phase in the aforementioned films may be constituted by any type of conductor, in particular:

(i) Experiments on amorphous thin W films [27] have shown the bulk T_c (12 mK [28]) can be increased by two orders of magnitude up to 2 or 3 K. It has been suggested [28] that this enhancement may be due to the presence of tungsten oxide having T_c close to 3 K. Another explanation of the enhanced superconductivity in amorphous W thin films might be derived from Ginzburg's surface-state superconductivity [29];

(ii) The tungsten–carbon compounds W_2C and W_xC_{1-x} for $0.45 < x < 0.5$ are superconductors showing a T_c in the range 2–10 K [30];

(iii) The tungsten–silicon compound $W_{0.6}Si_{0.4}$ is also a superconductor with a $T_c = 2.8$ K [27]. The superconducting incursions are most likely of the (ii) type since carbides have been detected that lead to critical temperatures of the main transitions as high as 3.9 K for certain W concentrations. At low W concentrations the samples show either one re-entrant peak or no peak at all. The samples with concentrations in the range 25–40 at.% manifest two re-entrant peaks; they have a room temperature resistivity in the range 10^5–10^3 $\mu\Omega$ cm.

3. Results of the critical current measurements

We carried out a series of measurements of the critical current I_c versus temperature in samples C–Si–W showing one or two re-entrant peaks (figures 1 and 2); in addition we measured and analysed the re-entrant peak resistance and the critical current versus temperature (figure 3) and the current–voltage characteristic (CVC) (figure 4) for the sample showing one peak. The behaviour of re-entrant resistance R versus temperature is shown in figures 1 and 2 (see [22]) for two typical samples with one and two peaks. The characteristic temperatures of these two sample are:

- The main superconducting transition temperature: $T_c = 3.49$ K;
- The Coulombian blockage temperature (temperature at peak's beginning): $T_b \simeq 2.25$ K;
- The temperature of the unblockage due to Josephson coupling: $T_{ub} \simeq 2.15$ K; for the sample showing one peak;
- The main superconducting transition temperature: $T_c = 3.43$ K;

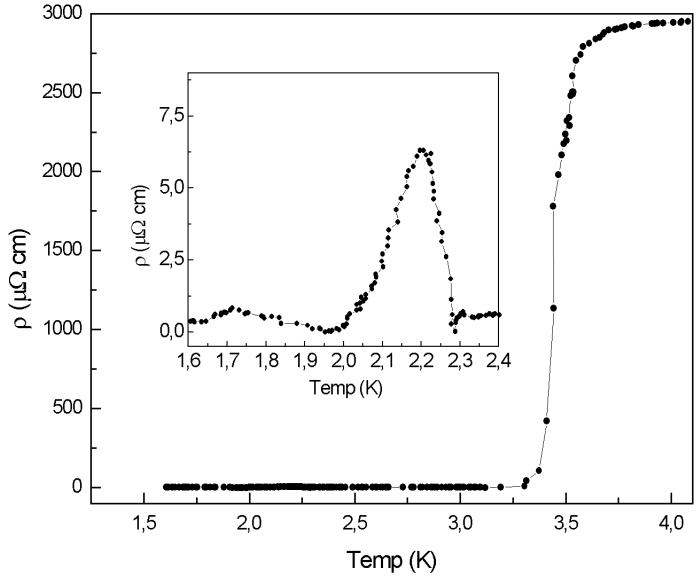

Figure 1. Main superconducting transition and typical re-entrant peak (inset) in one-peaked samples (sample no 1).

- The first Coulombian blockage temperature (temperature at first peak's beginning): $T_{b_1} \simeq 2.03$ K;
- The first Josephson unblockage temperature: $T_{ub_1} \simeq 1.95$ K;
- The second Coulombian blockage temperature (temperature at second peak's beginning): $T_{b_2} \simeq 1.71$ K;
- The second Josephson unblockage temperature: $T_{ub_2} \simeq 1.66$ K; for the sample showing two re-entrant peaks.

In some preceding papers of ours [22–26], devoted to the study of peak-like re-entrant transitions, we established:

(1) Re-entrant peaks show up as a single or two narrow ones ($\simeq$0.1 K wide) and in all samples peaks are observed at $T > 1$ K;
(2) Peaks are associated with the quasi-re-entrant superconducting phenomenon, i.e. the main superconducting transition is often incomplete, a non-zero resistance appearing in the temperature regions bounded by the main transition and the peaks themselves;
(3) The height of each peak is much smaller than the height of the main transition, being of the order of 10^{-3} R_n (some thousands of $\mu\Omega$ cm).

Note that the re-entrant peak (figures 1 and 2) is asymmetrical: the side corresponding to the Coulombian blockage (the one at higher temperature) is steeper than the one corresponding to unblockage due to Josephson coupling. This difference highlights that the blocking and unblocking mechanisms are intrinsically different and so is their dependence on temperature. Measurements of CVC show hysteresis phenomena. With increasing current a sudden appearance (jump) of a voltage takes place at a certain current value I_{c_1}, with decreasing current the voltage disappears at a lower current value than I_{c_2} and such that $I_{c_1} - I_{c_2} \simeq$ (0.2–0.5) mA (see the CVC with hysteresis measured in sample no 1 at $T = 3.26$ K, figure 4). The CVC under and near tension jumps is presented in figure 5 on a wider scale. The upgoing

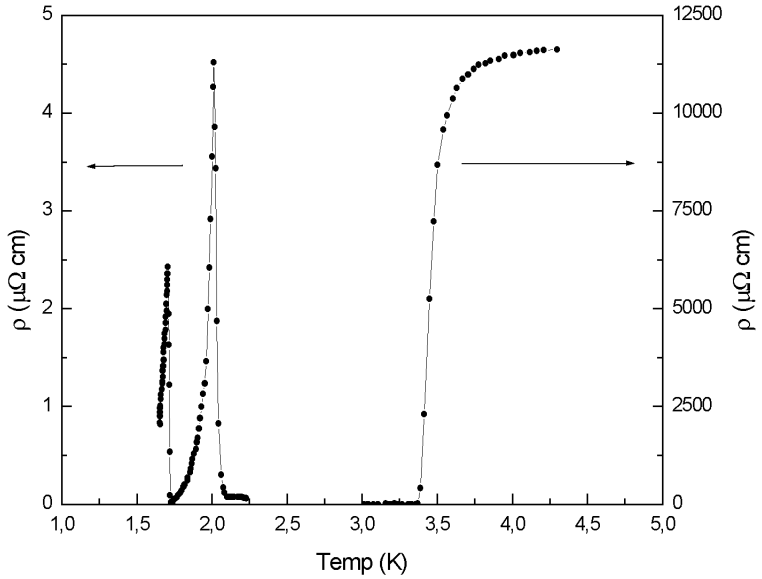

Figure 2. Main superconducting transition and typical re-entrant peaks in two-peaked samples (sample no 2).

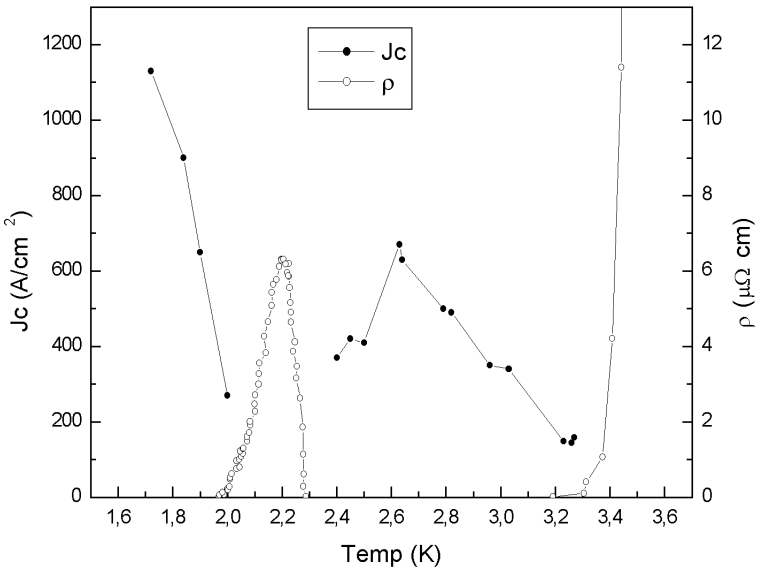

Figure 3. Re-entrant peak resistance (○) and critical current (●) versus temperature (sample no 1).

critical current dependence below and over the re-entrance peak is shown in figure 3 in which it can be seen that the critical current rapidly decreases near the re-entrance peak. CVC showing upward–downward inversion for $T \simeq 2.41$ K is shown in figures 6 and 7 on a larger and a smaller scale, respectively. It is possible to see that, before jumping, CVC begins to increase very rapidly (figures 5 and 7). The amplitude of the jump for upgoing temperature is 70–200 mV; over the jump the tension continues linearly increasing (the CVC corresponds to a

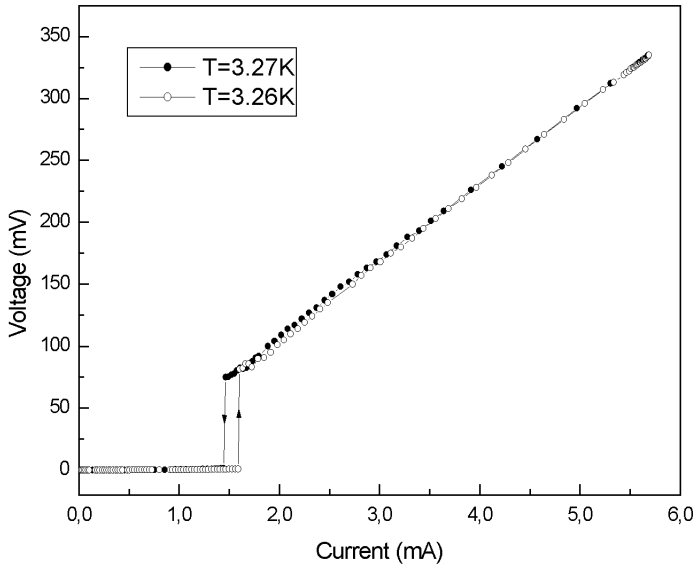

Figure 4. CVC in sample no 1 at $T_1 = 3.26\,\mathrm{K}$ (○) and $T_2 = 3.27\,\mathrm{K}$ (●). For currents $I_1 = 1.50\,\mathrm{mA}$ and $I_2 = 1.53$ mA jumps and hysteresis of CVC are observed.

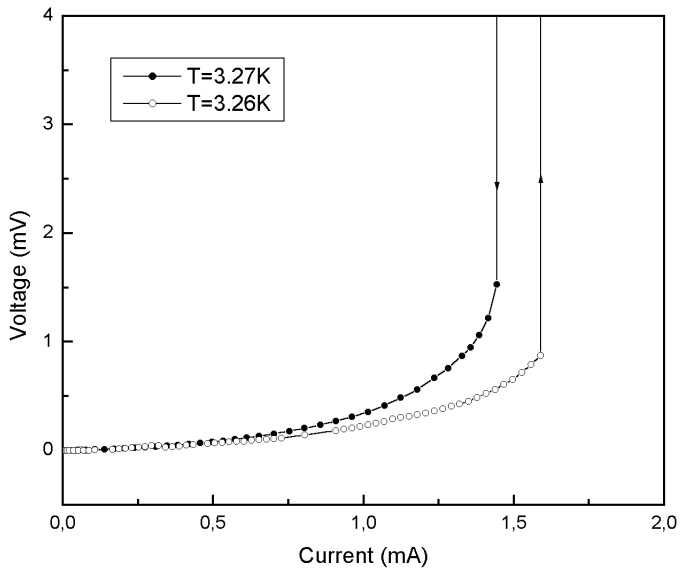

Figure 5. Same as figure 4 on a smaller scale. A sudden increase of tension and jumps are observed for a current value ∼1.5 mA.

CVC for ohmic conductance). In addition to hysteresis phenomena manifesting as voltage jumps in the CVC, measurements show the irreproducibility of the CVC and $I_c(T)$ curves in their small details: irreproducibility arises as a difference in values measured with upgoing or downgoing temperature, although showing a smaller order of amplitude with respect to the jumps in CVC.

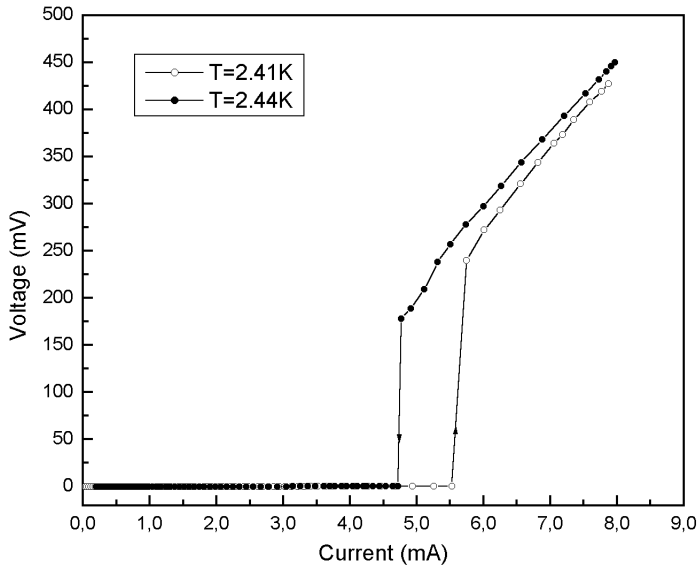

Figure 6. CVC showing hysteresis at $T \simeq 2.41$ K.

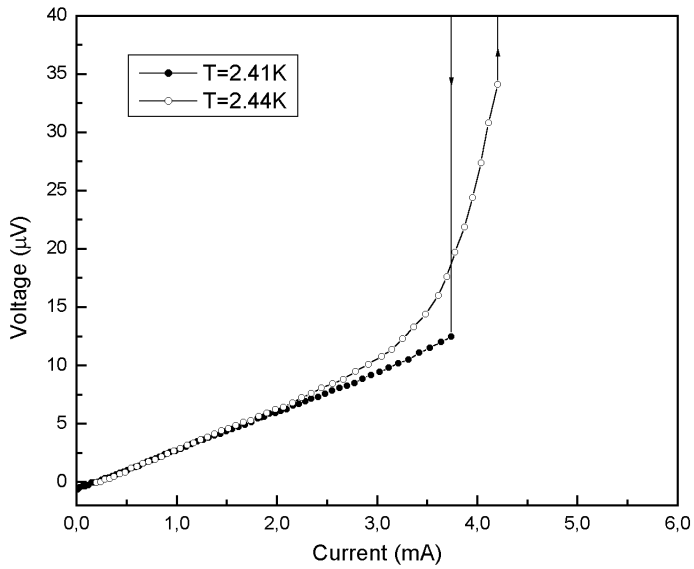

Figure 7. Part of CVC for sample no 1 near tension jumps for increasing and decreasing current at $T \simeq 2.41$ K.

4. Results. Numerical simulation for critical supercurrent

As the basis of the numerical simulations aimed to determine the critical supercurrent, we have generated several numerical samples representing a set of spherical, non-overlapping grains, with randomly distributed positions such that their radii and distances obeyed two Gaussian random distributions. Two main, different sets have been used to simulate samples with one or two distinct grain species. For the samples with one grain species we generated two random

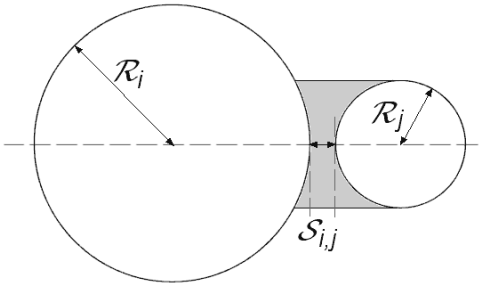

Figure 8. Two neighbouring superconducting grains in the dielectric matrix separated by the distance $S_{i,j}$ (Josephson junction in a granular superconductor).

Gaussian distributions for radii and intergranular distances characterized by mean values $\bar{R}$ and $\bar{\sigma}$ such that $\bar{R} = 220$ Å, $\bar{\delta} = 10$ Å with spread $3\sigma_R = 110$ Å and $3\sigma_\delta = 5$ Å, respectively; whereas for the samples with two grain species we generated two random Gaussian distributions for radii and one for the intergranular distances characterized by mean values $\bar{R}_1$, $\bar{R}_2$ and $\bar{\sigma}$ such that $\bar{R}_1 = 220$ Å, $\bar{R}_2 = 248$ Å, $\bar{\delta} = 10$ Å with spread $3\sigma_{R_1} = 110$, $3\sigma_{R_2} = 124$ and $3\sigma_\delta = 5$ Å, respectively. Once a simulation sample is generated, the critical current I_c is calculated by means of an algorithm searching for the maximum superconducting current that can flow through the macroscopical superconducting paths. Let us analyse the single Josephson junction for one pair of neighbouring grains with radii R^i and R^j, separated by a distance S_{ij} (figure 8). Since grains are spherical, it results that the dielectrical barrier between them is not constant. To describe such a barrier in a Josephson junction, Abeles [14] proposed to approximate it by a plane capacitor of section

$$\sigma = \pi\alpha(R_{\min}^{i,j})^2 \tag{3}$$

with $R_{\min}^{i,j} = \min\{R^i, R^j\}$ and the geometrical factor $\alpha \simeq 0.3$–0.6. This approximation is reasonable enough, since the maximal contribution to the tunnelling current given by Cooper pairs comes from the centre of the junction, where the barrier thickness is minimal. In this case the value S_{ij} represents the average thickness of the barrier (figure 8).

The critical supercurrent $I_c^{i,j}$ for a pair of grains i, j can be expressed by the following formula [31]

$$I_c^{i,j} = \frac{\pi}{2eR_N^{i,j}}\Delta(T)\tanh\left(\frac{\Delta(T)}{2k_BT}\right) = \frac{2e}{\hbar}E_J^{i,j} \tag{4}$$

(see formula (2)). The physical meaning of formula (4) may be explained using an equivalent expression

$$I_c^{i,j} = \frac{2e\sigma n_s\hbar}{m\delta}\,\mathrm{e}^{-S_{ij}/\delta} \tag{5}$$

where m is the mass of a single electron, n_s is the density of Cooper pairs in the superconducting grains and δ is the characteristic constant of the barrier between two grains defining its height U_0:

$$\delta = \frac{\hbar}{\sqrt{2mU_0}}. \tag{6}$$

It is known that both U_0 and σ are determined by the dielectric matrix in which the superconducting grains are immersed.

Typical values of I_c^{ij} vary in the range 1–100 μA [32]. Since *ab initio* computations for δ can determine only its magnitude order, the critical current computations, containing a factor $e^{-Sij/\delta}$, can only be determined with some approximation. However this factor contains the same value of the parameter δ for all junctions. It is known that in granular superconductors, near the Anderson transition, the determination of the actual value for δ is possible from a comparison of experimental values of the critical current with the results of numerical calculations; as a matter of fact the variation of δ in the tunnelling factor Sij/δ, due to different grain dimensions, is given by [40]

$$\frac{T_c}{T_{c_0}} = 1 - 0.48\frac{\varrho}{\varrho_m}\frac{k_B T_{c_0}}{\epsilon_F} \tag{7}$$

where T_{c_0} represent the critical temperature of the bulk as a whole, ϱ and ϱ_m represent Mott's resitivity and its maximal value, respectively, ϵ_F is the Fermi energy. Since it results

$$\frac{\Delta\delta}{\delta} = \frac{\Delta T_c}{T_{c_o}} \simeq \frac{k_B T_{c_o}}{\epsilon_F} \ll 1 \tag{8}$$

the same value δ can be taken for all grains.

The problem is then the calculation of the critical supercurrent I_c flowing through the whole simulated system. We define the critical current for a path as the smallest $I_c^{i,j}$ value for the grains pairs (i, j) forming it. Our definition for the critical current is justified by the fact we are interested in avoiding local transition into the dielectric state. Were all superconducting paths disjoint, the total critical current would simply be given by the sum of the critical currents through single paths. In general, though, paths intersect and share edges and/or nodes and the critical current flowing through the entire sample must be determined by maximizing the current passing through, while maintaining the superconducting state. This is physically reasonable, because the system tries to maintain the superconducting state as long as possible, for it is more convenient from an energetic point of view. The idea is, when crossed by a certain current, the system looks for all the possible paths to keep the global superconducting phase. The transition into the dielectric state starts locally only when all superconducting paths are saturated.

Thus, once the network connecting one electrode to the other is determined, the mathematical problem to be solved consists of the constrained maximization of the current that can be injected into one electrode and drained from the other one. The maximum critical current that can flow through the granular superconductor C–Si–W has been evaluated by means of computer simulations based on a model we developed to relate the re-entrance peaks to the absence of superconducting percolation paths joining the electrodes of our simulation samples [26].

The simulated samples have been generated as sets of non-overlapping spherical grains whose radii and relative distances obeyed Gaussian distributions. L_x, L_y, L_z being the dimensions of a sample, a number of grains proportional to the area $L_y L_z$, located in proximity of the plane $x = 0$ and an equal number of grains near the plane $x = L_x$ were considered to form the electrodes. A granular system, as a whole, is a superconductor at a given temperature if it is possible to transport Cooper pairs from one electrode to the other: this implies the existence of at least a percolation path over superconducting grains crossing the entire granular system. When paths are disjoint, the maximum critical current crossing the system consists of the sum of the maximum allowed critical current flowing through each single path; obviously the maximum supercurrent allowed to flow through a path corresponds to the minimum critical intergranular current $I_c^{i,j}$ on that path. In general, however, paths are not disjoint and the current flows through a complex network; the problem then must be solved by the determination of the maximum supercurrent injected by one electrode and drained from the other one such that each intergranular current $I_c^{i,j}$ is not exceeded. The first task performed by our simulations has

been the determination of the superconducting percolation paths—if any—running through the sample (connecting the electrodes) at a given temperature T; building a graph out of the sample has been accomplished by means of the association of a node to each grain and an edge to each pair of connected neighbouring grains, the connection condition for two neighbouring grains i, j being fulfilled if one of the conditions

$$k_B T \geqslant E_c^{i,j} \tag{9}$$

$$k_B T < E_c^{i,j} \qquad \text{and} \qquad z E_J^{i,j} > E_c^{i,j} + k_B T \tag{10}$$

holds.

In addition to obtaining detailed information on the paths, the process also allows us to build a network assigning each arc (i, j) a capacity equal to the critical current $I_c^{i,j}$ defined in equation (3). Then the determination of the maximum supercurrent through the system can be obtained solving a maximum net flow problem: given a network $\mathcal{G} = (\mathcal{N}, A)$ with non-negative capacities $u_{i,j}$ associated to each arc $(i, j) \in \mathcal{A}$, with $s, t \in \mathcal{N}$ the *source* and *terminal (drain)* node, respectively, then a flow v is determined such that:

$$\begin{aligned} &\textbf{max}\ v \\ &\sum_{\{j:(i,j)\in\mathcal{A}\}} x_{i,j} - \sum_{\{j:(i,j)\in\mathcal{A}\}} x_{j,i} = \begin{cases} 0 & \text{if} \quad i \in \mathcal{N} - \{s, t\} \\ -v & \text{if} \quad i = t \end{cases} \\ &0 \leqslant x_{i,j} \leqslant u_{i,j}. \end{aligned} \tag{11}$$

The correspondence between our granular system and the network has been built associating each grain to a node in $\mathcal{N}$, each pair of connected grains to an arc $(i, j) \in \mathcal{A}$, defining $u_{i,j} = I_c^{i,j}$ and introducing s and t as two fictitious nodes linked to all nodes belonging to the injection and drain electrode, respectively, by arcs of infinite capacity. The maximum critical current flow has then been obtained by the well known Ford–Fulkerson method [33] flanked by an '*ad hoc*' network reduction method developed to transform the network into a simpler, equivalent one. Results of the simulation for the critical current I_c versus temperature for the sample no 1 are shown in figure 9 (the scale for the current density was determined by comparison with experimental data for J_c). The simulation shows that the temperature range 2.0–2.2 K corresponds to the critical current $I_c = 0$. This range defines the position of the re-entrance peak on the temperature scale with rather good precision. The critical supercurrent $I_c(T)$, over and below the re-entrance peak, may be approximated by the function $I_c^{i,j}$ (see formula (4)). The simulation results for the critical current in sample no 2 having two re-entrance peaks are shown in figure 10. To perform such a simulation, we generated a sample made up of two types of superconducting grains whose radii were Gaussianly distributed around two different mean values $\bar{R}_1$ and $\bar{R}_2$. The single contributions of lower and higher critical temperatured grains are shown in figure 10(a) by solid and crossed curves; their total contribution is shown in figure 10(b). Note that in the temperature region below the second peak (the one at lower temperature) the conductive phase volume is larger and grows faster with decreasing temperature than the same volume both in the region between the two peaks and between the first peak and the main superconducting transition.

5. Discussion

First of all, let us pay attention to the good agreement, both qualitative and quantitative, between the experimental data and the results from the numerical simulation for the critical supercurrent. These results, together with the good agreement between the numerical study of the superconducting percolation paths and the positions of re-entrance peaks [26],

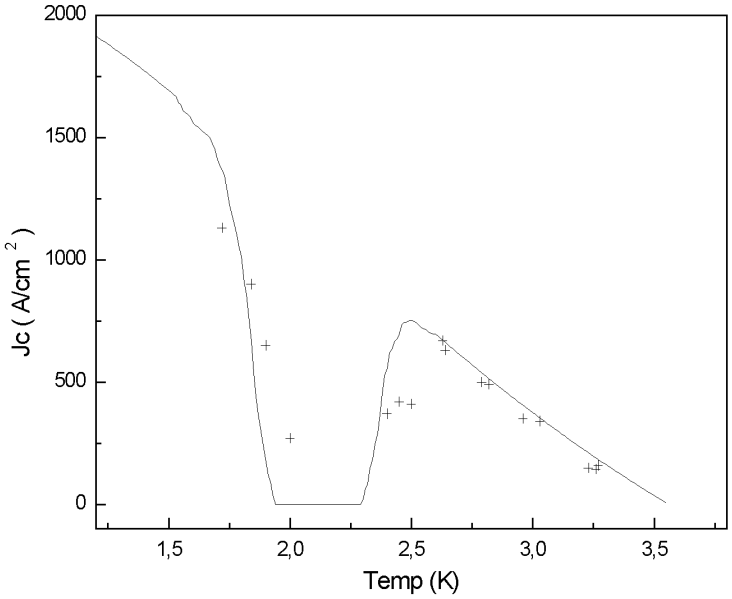

Figure 9. Numerical simulation results of the critical current versus temperature for sample no 1 (one re-entrance peak). The region around $T \sim 2$ K in which $I_c = 0$ corresponds to the re-entrance peak. Experimental data are also reported (+) for comparison.

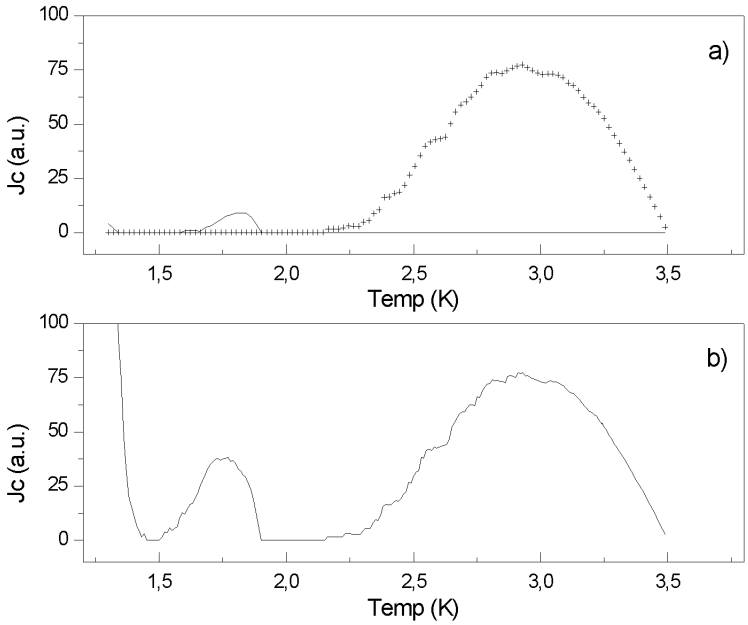

Figure 10. Numerical simulation results of the critical current versus temperature for sample no 2 (two re-entrance peaks). (a) Contributions from paths entirely formed from either first (solid line) or second type grains (crosses); (b) total grains network contribution to supercurrent. The intervals around $T \sim 2$ and 1.5 K in which $I_c = 0$ correspond to the first and the second re-entrance peaks.

led to the conclusion that the mechanisms proposed to explain the peaked re-entrant superconductivity phenomenon in C–Si–W adequately describe the actual situation in these granular superconductors. Note the difference between the simulation to determine the percolation paths through the macroscopical sample [26] and the simulation to determine the critical supercurrent. In fact, the simulation for the percolation paths regards the situation in which an infinitesimal supercurrent flows through the sample because the infinite cluster forms a superconducting shunt between the electrodes. The increase of the current leads to an immediate break of weak links of the cluster. In other words, the approach used in the simulation for the critical supercurrent has been the determination of the superconducting cluster using the maximum, finite value of the supercurrent for which the film is a superconductor; this implies the evaluation of the critical supercurrent through each Josephson junction of the sample. The determination of the critical supercurrent in the sample constitutes a richer characterization of the superconducting cluster in Si–C–W than the determination of the superconducting paths for an infinitesimal supercurrent. The results of critical supercurrent measurements and CVC for C–Si–W films at different temperatures are shown in figures 3–7 demonstrating a strong dependence on temperature (a strong dependence on the proximity of the peak). To analyse the experimental data we suppose that the C–Si–W films are disordered JJA made up of a great number of Josephson contacts between close grains. The CVC of a set of junctions [34] can be reduced to the CVC of a single Josephson junction in such a way that it is equivalent to JJA of the C–Si–W film. From Josephson effect theory [34–38] it is known that its description is usually provided by the RCSJ (resistively and capacitively shunted junction) model in which a physical Josephson junction is represented by an ideal one described by the equation

$$I = I_{c_0} \sin \varphi \tag{12}$$

where φ is the the phase difference across the barrier and I_{c_0} the maximum critical current shunted by an impedance R_N and a capacitance C (figures 11(a), (b)). The impedance R_N accounts for dissipation in the finite voltage regime without affecting the lossless dc regime, where C reflects the geometric shunting capacitance between two electrodes. The derivation of the tunnelling current was given by Josephson [35] and was reviewed by Barone e Paternò [36]; for a constant dc bias V_0 the result is:

$$I = I_0(V_0, T) \sin \varphi + [\sigma_0(V_0, T) + \sigma_1(V_0, T) \cos \varphi] V_0. \tag{13}$$

The second term in equation (13) results from quasi-particle tunnelling and may be described as a normal current in parallel with the supercurrent. Within the RCSJ model, the time dependence of the phase φ in the presence of an extremely supplied bias current can be derived by equating the bias current I to the total junction current from the three parallel channels as follows [37]:

$$I = I_{c_0} \sin \varphi + V/R_N + C \frac{\mathrm{d}V}{\mathrm{d}t}. \tag{14}$$

In this equation I_{c_0} has been introduced as a coefficient of $\sin \varphi$, the notation I_c denoting an observable critical current. Equation (14) is equivalent to the second-order differential equation

$$\frac{\mathrm{d}^2\varphi}{\mathrm{d}\tau^2} + \frac{1}{Q} \frac{\mathrm{d}\varphi}{\mathrm{d}\tau} + \sin \varphi = I/I_{c_0} \tag{15}$$

where τ is a dimensionless time variable $\tau = \omega_p t$ with

$$\omega_p = \left(\frac{2eI_{c_0}}{\hbar C} \right)^{1/2} \tag{16}$$

being the so-called plasma frequency of the junction and Q is the 'quality' factor:

$$Q = \omega_p R_N C \tag{17}$$

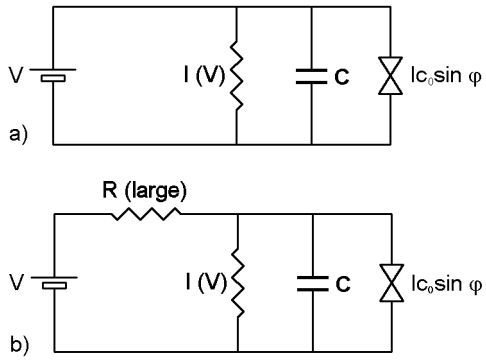

Figure 11. Resistive model circuits for Josephson and ohmic current: (a) voltage feed regime, (b) current feed regime.

where the parameter Q is identical to $\beta_c^{1/2}$ where β_c is a frequency parameter introduced by Stewart [38] and Mc Cumber [39]. Let us now analyse the influence of circuit parameters on the CVC for dc regimes. In general there are two factors involved: the nature of the external circuit driving the junction, and the form of the background current which the junction would carry in the absence of a supercurrent. We write the background current as $I_N(V)$ and assume it is in parallel with the Josephson current, so that the governing equations are:

$$I = I_{c_0} \sin\varphi + I_N(V) \tag{18}$$

$$\hbar \frac{\mathrm{d}\varphi}{\mathrm{d}t} = 2\,\mathrm{eV}. \tag{19}$$

There are two extreme forms of external circuit conditions: voltage feed and current feed. With voltage feed (figure 11(a)), V is fixed and the current to be determined, whereas with current feed (figure 11(b)), the current is fixed and V is to be determined. Experiments generally use current feed, since the dc impedance of the junction is low. It is also possible to simplify the problem by taking the background current as ohmic

$$I_N = G_N V \tag{20}$$

where G_N is the normal conductance of the junction. On the other hand, for current feed, φ is no longer linear in time and consequently $I_{c_0} \sin\varphi$ does not average to zero. Since I is fixed, the substitution for V in (17) using (18) gives

$$\frac{\hbar}{2e} G_N \frac{\mathrm{d}\varphi}{\mathrm{d}t} + I_{c_0} \sin\varphi = I_N(V) \tag{21}$$

where $I_N(V)$ is ohmic. From the time average of $\mathrm{d}\varphi/\mathrm{d}t$, the result is [38, 39]:

$$(G_{nN} V_{\mathrm{dc}})^2 + I_{c_0}^2 = I^2. \tag{22}$$

Equation (22) describes the CVC for the current feed regime (see figure 11(b)). As I increases, V_{dc} gradually approaches the background value. The parameter β_c that enters the CVC description in the current-fed regime (see figure 12) is the reduced capacitance:

$$\beta_c = \frac{2e I_{c_0} C_{\beta_c}}{\hbar G_N^2}. \tag{23}$$

As shown in figures 4–7 the CVC obtained from critical current measurements in C–Si–W films are similar to the CVC of the Josephson contact in the current-fed regime. It is worth noticing that these CVC show hysteresis phenomena too [38]. All this allows us to conclude that

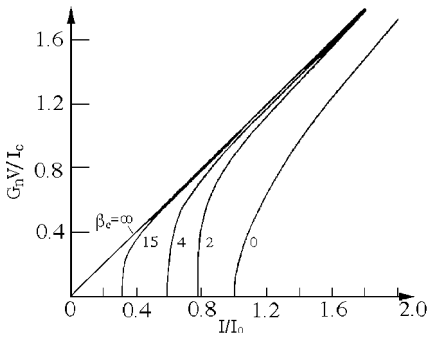

Figure 12. CVC for a current-fed junction with a capacitance in parallel. Note that current is plotted along the horizontal axis. Each curve is labeled by the corresponding value of β_c, where β_c is the capacitance in reduced units: $\beta_c = 2eI_{c_0}C_{\beta_c}/\hbar G_N^2$.

the C–Si–W films under examination—constituted by a large number of Josephson junctions connected in a disordered way—can be represented by an equivalent single junction with well defined parameters I_{c_0}, β_c, G_N, C with I_{c_0} the critical current, $1/G_N$ the normal impedance, and the constant $C_{\beta_c} \cdot 1/G_N$ describing the characteristic time of response to the perturbation. Let us evaluate the average capacitance $\bar{C}$ using the plane capacitor approximation for an average Josephson junction constituted by two grains [26]:

$$\bar{C}_p = \alpha\pi \frac{\epsilon_0\epsilon_r}{\bar{S}_{ij}} \bar{R}_i^2. \tag{24}$$

Taking average values for C–Si–W films from [26]: $\epsilon_0 = 8.85 \times 10^{-12}$ C^2 N^{-1} m^{-2}, $\epsilon_r = 19$, $\bar{R}_i = 220$ Å, $\bar{S}_{i,j} = 10$ Å, $\alpha = 0.5$, it results:

$$\bar{C}_p = 1.27 \times 10^{-16} \text{ F}. \tag{25}$$

Let us evaluate the equivalent capacitance C_{β_c} using experimental parameters for CVC in C–Si–W films and formula (23). Using the experimental parameters for sample no 1 ($I_{c_0} = 1.5$ mA, $V_{\text{dc}} = 75$ mV, $R_N = V_{\text{dc}}/I_0 = 50\ \Omega$) we obtain $C_{\beta_c} = 0.88 \times 10^{-16}\ \beta_c$ F while using formula (23) and typical values for sample no 1: $I_0 = 1.5 \times 10^{-3}$ A, $V_{\text{dc}} = 75 \times 10^{-3}$ V, $R_n = V_{\text{dc}}/I_0 = 50\ \Omega$, we obtain:

$$C_{\beta_c} = 0.9 \times 10^{-16}\beta_c \text{ F}. \tag{26}$$

The dimensionless parameter β_c for a similar CVC in figure 11 is equal to 2–4. From the comparison of the CVC for the film C–Si–W and the one for a single Josephson junction results a surprising consequence: the capacitance $\bar{C}_p$ of the single Josephson contact is practically the same order of magnitude as the equivalent capacitance of a large number of Josephson contacts linked in a JJA. At the same time the impedance R_N of the single contact is ∼15–30 KΩ (see [26]) and exceeds the equivalent impedance for the JJA in the C–Si–W by $\sim 10^3$ times. It is obvious that the equivalent parameters in the JJA depend on the kind of connections of a large number of Josephson junctions in the film where impedance and capacitance for different single contacts can be connected either in series or in parallel with respect to supercurrent direction in JJA. The relation $C_p \sim C_{\beta_c}$ may demonstrate that the probabilities of parallel and serial capacitance connections are the same, whereas for the impedance of a single junction the higher probability is obtained for the parallel connection. Let us finally calculate the magnitude of the Q parameter that allows us to characterize the type of Josephson junctions obtained in granular superconductor films C–Si–W. It is known [36] that for $Q \gg 1$ the CVC

of the Josephson contact becomes hysteresic; this can be observed in the CVC of C–Si–W film samples. Let us evaluate the Q for the C–Si–W samples presented in this paper. The plasma frequency (16) for sample no 1 is $\omega_p = 2.1 \times 10^{14}$ Hz; using the relation $Q = \omega_p R_n C$ and $R_N \simeq 5 \times 10^4\ \Omega$, $C \simeq \beta_c \times 10^{-16}$ F, it results $Q \sim 10^3 \gg 1$. According to Tinkam [37] this means that Josephson junctions in C–Si–W films are underdamped junctions with the CVC of the hysteresic type. The equivalent impedance decrease is in agreement with the increase of the critical current I_{c_0} that characterizes the JJA of the film. This value of I_{c_0} (for parallel junctions) is much larger than the average critical current for a single junction. It is also possible to estimate the time constant T for a single contact and for the whole system of junctions in the C–Si–W; taking $C \simeq 10^{-16}$ F and $R_N \simeq 50\ \Omega$ for the JJA and $R_N \simeq 2 \times 10^3\ \Omega$ for a single contact, we obtain $T_{\text{single}} \simeq 2 \times 10^{-13}$ s and $T_{\text{JJA}} \simeq 5 \times 10^{-15}$ s: the charge diffusion in JJA occurs 10^2 times faster than in the single contact and this difference is completely due to the higher value of the impedance for a single Josephson contact.

6. Conclusions

We have experimentally studied the critical supercurrent I_{c_0} and the CVC in granular superconductors C–Si–W in which a peak-type re-entrant superconductivity is observed. I_{c_0} and CVC measurements have been carried out on samples showing one or two re-entrance peaks. The dependence of the critical current on temperature has been analysed in the intervals between the main transition and the first peak, between the first and the second peak, and below the second peak; it resulted that both I_{c_0} and CVC are non-reproducible and manifest hysteresis phenomena on a mesoscopical scale. We have developed a simulation model for the critical current as a function of temperature and showed the good agreement of the simulation results with the experimental data from the samples with one or two re-entrance peaks. We, finally, have determined all basic parameters: critical current I_{c_0}, plasma frequency ω_p, single contact capacitance C, quality factor Q, normal impedance R_N for a single junction, time constant T. We also proposed an hypothesis of connection for single junctions and analysed the possibility of equating the capacitance of a single junction to the characteristic capacitance of the whole JJA.

References

[1] Bulaevskii L N, Buzdin A I, Kulic M L and Panjukov S V 1982 *Adv. Phys.* **8** 115
[2] Morozov Yu G, Naumenko I G and Petinov V I 1976 *Sov. J. Low-Temp. Phys.* **2** 484
[3] Belevtsev B I, Komnik Yu F and Fomin A V 1987 *J. Low Temp. Phys.* **69** 401
[4] Abeles B, Sheng P, Goutts M D and Arie Y 1975 *Adv. Phys.* **24** 406
[5] Sheng P 1992 *Phil. Mag.* B **65** 357
[6] Pollak M and Adkins C J 1992 *Phil. Mag.* B **65** 267
[7] Hebard A F and Paalanen M A 1984 *Phys. Rev.* B **30** 4063
[8] Kunchur M, Lindenfeld P, McLean W L and Brooks J S 1987 *Phys. Rev. Lett.* **59** 1232
[9] Kobayashi S, Tada Y and Sasaki W 1981 *Physica* B **107** 129
[10] Glukhov A M, Dmitrienko I M and Shablo A A 1983 *Sov. J. Low-Temp. Phys.* **9** 13
[11] Dynes R C, Garno J P and Rowel J M 1978 *Phys. Rev. Lett.* **40** 479
[12] White A E, Dynes R C and Garno J P 1986 *Phys. Rev.* B **33** 3549
[13] Jaeger H M, Haviland D B, Goldman A M and Orr B G 1986 *Phys. Rev.* B **34** 4920
[14] Abeles B 1977 *Phys. Rev.* B **15** 2828
[15] Šimanek E 1979 *Solid State Commun.* **31** 419
[16] Efetov K B 1980 *Sov. Phys.–JETP* **68** 2017
[17] Grignani G, Mattoni A, Sodano P and Trombettoni A 1999 *Preprint* cond-mat/9902183
[18] Mooji J E, van Wees B J, Geerligs L J, Peters M, Fazio R and Schön G 1990 *Phys. Rev. Lett.* **65** 645
[19] van der Zant H S J, Elion W J, Geerligs L J and Mooji J E 1996 *Phys. Rev.* B **54** 10 081

[20] Dorfman V F and Pypkin B N 1991 *Surf. Coat. Technol.* **49** 193
[21] Dorfman V F 1992 *Thin Solid Films* **212** 267
[22] Bozhko A D, Chudinov S M, Rodichev D Yu, Pypkin B N, Stizza S and Berrettoni M 1993 *Phys. Status Solidi* b **177** 475
[23] Berrettoni M, Bozhko A, Briggs A, Chudinov S M, Pypkin B N and Stizza S 1995 *Condens. Matter Mater. Commun.* **2** 71
[24] Bozhko A, Chudinov S M, Stizza S, Pypkin B and Shuppegin M 1998 *J. Phys.: Condens. Matter* **10** 1855
[25] Bozhko A, Chudinov S M, Rodichev D Yu, Pypkin B N, Stizza S and Pypkin B 1997 *Phys. Status Solidi* b **199** 197
[26] Chudinov S M, Ferretti R, Fusari S, Mancini G and Stizza S 2000 *Phys. Rev.* B **62** 12 516
[27] Bond W L, Cooper A S, Andres K, Hull G W, Geballe T M and Matthias B T 1965 *Phys. Rev. Lett.* **15** 260
[28] Gibson J W and Matthias B T 1965 *Phys. Rev. Lett.* **15** 260
Gibson J W and Matthias B T 1964 *Phys. Rev. Lett.* **12** 688
[29] Ginzburg V L 1964 *Phys. Lett.* **13** 201
[30] Roberts W B 1976 *J. Phys. Chem.* **5** 581
[31] Ambegaokar V and Baratoff A 1963 *Phys. Rev. Lett.* **10** 468
Ambegaokar V and Baratoff A 1963 *Phys. Rev. Lett.* **11** 104
[32] Lounasmaa O V 1974 *Experimental Principles and Methods Below 1 K* (London: Academic)
[33] Ford L R Jr and Fulkerson D R 1956 *Can. J. Math.* **8** 399
Ford L R Jr and Fulkerson D R 1957 *Can. J. Math.* **9** 210
[34] Tilliy D and Tilliy J 1994 *Superfluidity and Superconductivity (Graduate Student Series in Physics)* (Bristol: J W Arrowsmith) p 263
[35] Josephson B 1965 *Phys. Lett.* **1** 251
[36] Barone A and Paternò G 1984 *Physics and the Application of the Josephson Effect* (New York: Wiley-Interscience)
[37] Tinkham M 1996 *Introduction to Superconductivity (Int. Series in Pure Appl. Phys.)* 2nd edn (New York: McGraw-Hill)
[38] Stewart W 1968 *Appl. Phys. Lett.* **12** 277
[39] Mc Cumber D 1968 *J. Appl. Phys.* **39** 3113
[40] Belevtsev B I 1990 *Sov. Usp. Fiz. Nauk* **160** 65